ISSN 2616-5767 Vol.9, Issue 4: 82-89, DOI: 10.25236/AJETS.2026.090410

Research on Surface Defect Detection Technology of Corrugated Beam Steel Guardrails Based on a Vehicle-Mounted Vision System

Qiu Lin

China Merchants Chongqing Testing Center for Highway Engineering Co., Ltd., Chongqing, 400067, China
qlove666888@126.com

Abstract: *Corrugated beam steel guardrails are critical facilities for highway traffic safety. Surface defects such as panel deformation, missing bolts, and post inclination directly threaten highway operation safety. Traditional manual inspection methods suffer from low efficiency and insufficient accuracy, making them difficult to satisfy the requirements of large-scale highway monitoring. Therefore, this study investigates a surface defect detection technology for guardrails based on a vehicle-mounted vision system. A vehicle-mounted vision system consisting of multiple line-scan cameras, an area-scan camera, a rotary encoder, and a GPS positioning device was designed. Multi-view imaging configurations were adopted to acquire images of different guardrail components. Based on this system, a detection method incorporating image preprocessing and identification of various critical defects was proposed. By utilizing contour recognition and color comparison techniques, accurate identification and localization of defects were achieved, providing reliable technical support for highway guardrail safety monitoring.*

Keywords: *steel guardrail; vehicle-mounted vision; surface defect; detection technology*

1. Introduction

Corrugated beam steel guardrails mainly consist of guardrail panels, posts, blockouts, and bolts. The surface color is generally uniform pure silver, pure green, or pure blue, and their shapes and dimensions shall comply with the requirements specified in national standards. Guardrail panels can be classified into two types: two-wave guardrail panels and three-wave guardrail panels. The heads of bolts installed on guardrail panels are circular, and rectangular washers can be additionally installed during bolt installation [1].

Posts can be divided into circular tube posts and square tube posts. The numbers of connecting bolts between posts and blockouts are one and two, respectively. A circular post is also equipped with a circular post cap at its top.

In recent years, the Ministry of Transport has continuously conducted technical condition monitoring and evaluation of traffic safety facilities within the national highway network. Highway operation and management organizations also regularly perform safety hazard inspections and typical defect identification of in-service corrugated beam steel guardrails. Surface defects of corrugated beam steel guardrails include poor alignment comfort, panel deformation and damage, minor dents/protrusions, scratches, corrosion, post inclination, missing post caps, and missing or loose bolts [2]. Among these defects, panel deformation damage and missing bolts have the greatest impact on the mechanical safety performance of guardrails.

2. Current Status of Intelligent Guardrail Inspection Technology

To address the problems associated with traditional highway guardrail inspection, including reliance on manual inspections conducted on foot, high inspection costs, and long inspection cycles, Ma Shanyong et al. developed an intelligent diagnostic system for expressway guardrail defects [1]. With a lightweight edge-deployed large model as its core, the system integrates fixed video surveillance and vehicle-mounted mobile data acquisition to achieve automatic identification and early warning of guardrail defects, such as damage, corrosion, and missing bolts, as well as collision events, with a defect

ISSN 2616-5767 Vol.9, Issue 4: 82-89, DOI: 10.25236/AJETS.2026.090410

identification accuracy exceeding 90%. Li Zhixiong et al. proposed a lightweight attention-enhanced YOLOv8 algorithm for missing bolt detection in corrugated beam steel guardrails. The algorithm adopts MobileNetV3 as the backbone network and introduces the C2f module to enhance feature reuse and multi-scale feature representation capabilities [2]. Images of guardrail bolts were acquired using a guardrail inspection robot in both laboratory and real-world expressway environments, and field tests demonstrated a detection accuracy of up to 97.48%.

Wei Li et al. developed a rapid detection technology for assessing the extent of damage to expressway corrugated beam guardrails [3]. The proposed multi-sensor fusion system integrates a high-dynamic-range camera, solid-state LiDAR, a BeiDou positioning module, and an inertial measurement unit (IMU). By adopting an integrated "perception–acquisition–analysis" architecture, the system enables automated, non-contact detection of six types of typical defects, including guardrail corrosion and missing bolts. Wang Huifeng et al. investigated a vehicle-mounted structured-light scanning inspection system based on an autonomous mobile robot platform and developed algorithms suitable for measuring the crossbeam center height, panel profile, deformation, and inclination of corrugated beam guardrails [4]. The measurement errors of the crossbeam center height for both two-wave and three-wave guardrail panels were strictly controlled within 4 mm, while the accuracy of panel deformation detection exceeded 80%.

Li Shuang analyzed the damage types of expressway corrugated beam guardrails and proposed a data acquisition scheme integrating high-resolution image sensors, infrared thermal imaging sensors, and acceleration sensors [5], enabling automatic identification of damage such as cracks, deformation, and corrosion. Li Jia designed a vision-based damage detection system for expressway corrugated beam guardrails [6] and proposed a target tracking and detection algorithm for corrugated beam guardrail regions. Edge detection, line fitting, and other techniques were employed to detect and identify abnormal guardrail appearances, and experiments and analyses were conducted on the functional modules of the corrugated beam guardrail damage detection system.

In addition, regarding continuous monitoring of highway guardrail conditions, Yang Man et al. utilized existing fixed video acquisition facilities along highways and applied machine vision analysis technology to achieve real-time detection and early warning of abnormal conditions, such as guardrail damage and collisions [7]. They also conducted a pilot application of an intelligent highway guardrail condition monitoring system based on machine vision.

3. Vehicle-Mounted Vision System

The typical composition of a two-wave corrugated beam steel guardrail is shown in Fig. 1. To acquire images of surface defects of two-wave and three-wave corrugated beam steel guardrails, a vehicle-mounted vision system scheme was proposed.

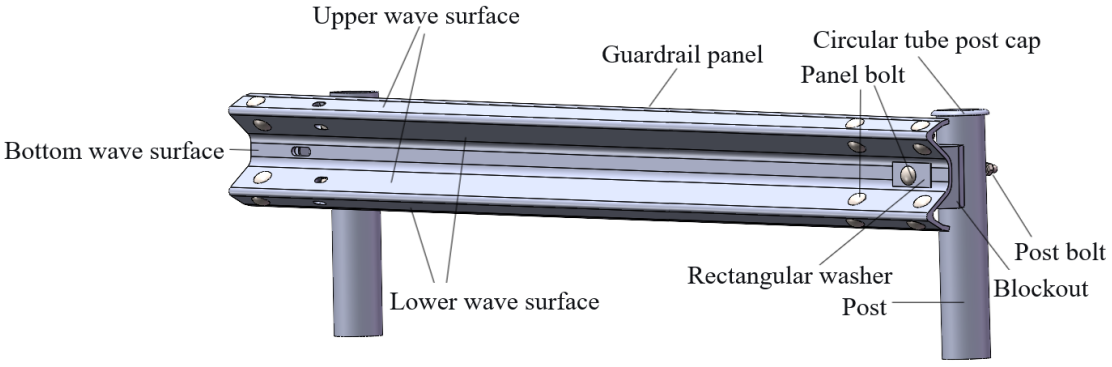
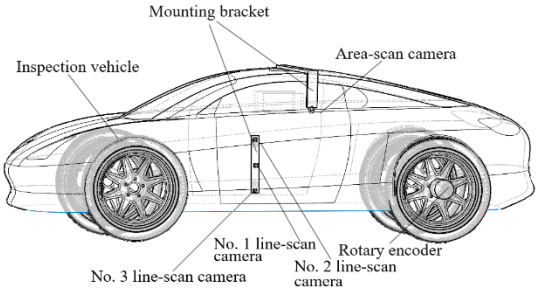


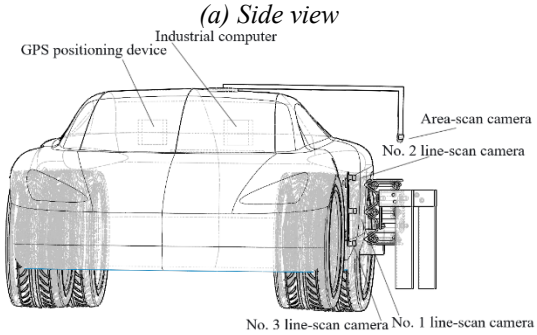
Fig. 1 Schematic diagram of the composition of a typical two-wave corrugated beam steel guardrail

The vehicle-mounted vision system consists of three line-scan cameras, an area-scan camera, a rotary encoder, a GPS positioning device, an industrial computer, mounting brackets, and an inspection vehicle, as shown in Fig. 2.

ISSN 2616-5767 Vol.9, Issue 4: 82-89, DOI: 10.25236/AJETS.2026.090410



(a) Side view



(b) Front view

Fig. 2 Schematic diagram of the composition of the vehicle-mounted vision system

Both the line-scan cameras and the area-scan camera are full-color cameras, which are connected to the side and top of the inspection vehicle body through mounting brackets. The installation height of the No. 1 line-scan camera is approximately the same as the center height of the roadside guardrail panel (approximately 65 cm above the road surface). After installation, the scanning line is perpendicular to the road surface and is used to acquire images of the guardrail panel and post from the front view.

The installation heights of the No. 2 and No. 3 line-scan cameras are higher than the top of the guardrail panel and lower than the bottom of the guardrail panel, respectively. After installation, the projections of their scanning lines on the road surface are both perpendicular to the driving direction. They are used to acquire images of the guardrail panel from the top-view and bottom-view perspectives, respectively.

The installation height of the area-scan camera is higher than the top of the guardrail panel, and its projection on the ground is located outside the guardrail. After installation, the central optical axis is parallel to the driving direction and intersects the ground at an acute angle. It is used to acquire images of the external posts of the guardrail and their bolts.

The rotary encoder is installed at the center of the rear wheel hub of the inspection vehicle and is used to detect changes in the position of the inspection vehicle and trigger image acquisition by the line-scan cameras and area-scan camera. The GPS positioning device is installed inside the inspection vehicle to obtain real-time position information of the vehicle. The industrial computer is used to control image and position acquisition, as well as to perform identification and analysis of guardrail surface defects.

4. Surface Defect Detection Method

4.1 Image Acquisition and Preprocessing

According to the spatial relationships among the imaging fields of view of the No. 1, No. 2, and No. 3 line-scan cameras, mapping functions were established in advance for two-wave and three-wave guardrail panels, respectively. The positions of the top and bottom edges of the guardrail panel in the image captured by the No. 1 camera were used as inputs. The output consisted of the mapping functions F_{bd}, F_{sb}, and F_{xb}, which corresponded to the bottom wave surface sub-image of the guardrail panel in the No. 1 camera image, the upper wave surface sub-image in the No. 2 camera image, and the lower wave surface sub-image in the No. 3 camera image, respectively.

The inspection vehicle was controlled so that the distance between the vehicle-mounted inspection device and the inspected guardrail remained within a specified range. The line-scan cameras and area-scan camera continuously acquired images Img1, Img2, Img3, and ImgM, respectively, while the GPS

ISSN 2616-5767 Vol.9, Issue 4: 82-89, DOI: 10.25236/AJETS.2026.090410

positioning device continuously collected the position information of the inspection vehicle.

The images Img1, Img2, and Img3 were rotated so that the longitudinal direction of the guardrail panel in the images was consistent with the horizontal direction, and the top edge of the guardrail panel was located above the bottom edge. Subsequently, grayscale conversion, edge detection, binarization, and dilation/erosion operations were sequentially performed on Img1, Img2, and Img3, producing the processed images $Img1_{edge}$, $Img2_{edge}$, and $Img3_{edge}$

All line segments with lengths greater than a specified threshold were identified in $Img1_{edge}$. The uppermost and lowermost line segments were defined as L_{top} and L_{bot}, respectively. The pixel distance between L_{top} and L_{bot} in $Img1_{edge}$ was used to determine whether the guardrail panel was a two-wave or three-wave guardrail panel.

Meanwhile, according to the positions of L_{top} and L_{bot}, the bottom wave surface sub-images ROI_{bd} and $ROI_{edge-bd}$ were extracted from Img1 and $Img1_{edge}$ using F_{bd}. The upper wave surface sub-images ROI_{sb} and $ROI_{edge-sb}$ were extracted from Img2 and $Img2_{edge}$ using F_{sb}. The lower wave surface sub-images ROI_{xb} and $ROI_{edge-xb}$ were extracted from Img3 and $Img3_{edge}$ using F_{xb}.

For ImgM, grayscale conversion, edge detection, binarization, and dilation/erosion operations were sequentially performed to obtain $ImgM_{edge}$. Two vertical parallel lines L_{left} and L_{right} satisfying specific requirements for length and spacing were identified in $ImgM_{edge}$. Circular or elliptical contours meeting the required dimensions were searched for in the region above L_{left} and L_{right}. If such contours existed, the post was determined to be a circular tube post; otherwise, it was determined to be a square tube post.

4.2 Guardrail Panel Bolt Missing Detection

The missing bolts on the bottom wave surface of the guardrail panel were detected from ROI_{bd} and $ROI_{edge-bd}$ according to the following steps:

Step 1: Identify all circular contours and elliptical contours in $ROI_{edge-bd}$.

Step 2: For any circular contour, determine whether there exists a rectangular contour of a specified size centered at the circle center and containing the circular contour. If yes, proceed to Step 3; otherwise, proceed to Step 4.

Step 3: Determine whether the color inside the circular contour in ROI_{bd} is consistent with the color inside the rectangular contour outside the circular contour. If yes, the bolt at the position of the circular contour is determined to be not missing. If not, the bolt at the position of the circular contour is determined to be missing, and its position information is recorded. Then proceed to Step 5.

Step 4: Determine whether a complete elliptical contour exists in the region of the circular contour, with the circular contour contained within the elliptical contour. If yes, the bolt at the position of the circular contour is determined to be missing, and its position information is recorded. Otherwise, the bolt at the position of the circular contour is determined to be not missing.

Step 5: Repeat Steps 2–4 for the next circular contour until all circular contours have been processed.

Similarly, the missing bolts on the upper wave surface of the guardrail panel are detected from ROI_{sb} and $ROI_{edge-sb}$, and the missing bolts on the lower wave surface of the guardrail panel are detected from ROI_{xb} and $ROI_{edge-xb}$.

4.3 Guardrail Panel Top/Bottom Edge Deformation Damage Detection

The deformation damage of the top edge of the guardrail panel was detected from ROI_{bd} and $ROI_{edge-bd}$ according to the following steps:

Step 1: Determine whether L_{top} horizontally traverses the entire image in $ROI_{edge-bd}$. If yes, the top edge of the guardrail panel is considered normal, and the process is terminated. Otherwise, proceed to Step 2.

Step 2: Extend L_{top} until it horizontally traverses the entire image, connect L_{top} with other contours within a certain region above and below it, and obtain several closed contours satisfying the required size conditions.

Step 3: For any closed contour above L_{top}, determine whether the color inside the contour in ROI_{bd} is consistent with the color in the region below L_{top} outside the contour. If yes, the top edge of the guardrail

ISSN 2616-5767 Vol.9, Issue 4: 82-89, DOI: 10.25236/AJETS.2026.090410

panel is determined to have deformation damage, and the position information is recorded. Otherwise, the top edge of the guardrail panel at this contour location is considered normal. Then proceed to Step 5.

Step 4: For any closed contour below L_{top}, determine whether the color inside the contour in ROI_{bd} is consistent with the color in the left and right regions outside the contour. If yes, the top edge of the guardrail panel at this contour location is considered normal. Otherwise, the top edge of the guardrail panel is determined to have deformation damage, and the position information is recorded.

Step 5: Repeat Steps 3–4 for the next closed contour until all closed contours have been processed.

Similarly, the deformation damage of the bottom edge of the guardrail panel is detected from ROI_{bd} and $ROI_{edge\text{-}bd}$.

4.4 Internal Deformation Damage Detection of Guardrail Panel Surface

The internal deformation damage of the guardrail panel surface was detected from ROI_{bd} and $ROI_{edge\text{-}bd}$ according to the following steps:

Step 1: For all line segments between L_{top} and L_{bot}, determine whether they all horizontally traverse the entire image. If yes, the internal region of the guardrail panel surface is considered normal, and the process is terminated. Otherwise, proceed to Step 2.

Step 2: For any line segment L_k between L_{top} and L_{bot}, connect the endpoints of L_k with nearby contours and determine whether closed contours exist. If yes, the guardrail panel surface is determined to have internal deformation damage, and the position information is recorded. Then proceed to Step 5. Otherwise, proceed to Step 3.

Step 3: Extract weak edges in the region near the endpoints of L_k in ROI_{bd}.

Step 4: Determine whether the weak edges contain line segments connected with the endpoints of L_k. If yes, the guardrail panel surface at the corresponding line segment is considered normal. Otherwise, the guardrail panel surface is determined to have internal deformation damage, and the position information is recorded.

Step 5: Repeat Steps 2–4 for the next line segment until all line segments have been processed.

4.5 Post Bolt Detection

For circular tube posts, the missing bolts were detected from $ImgM_{edge}$ according to the following steps:

Step 1: If ImgM is an image of a guardrail post located on the left side of the driving direction, L_{left} is selected as the reference line; otherwise, L_{right} is selected as the reference line.

Step 2: Search for closed contours connected with L_{left} or L_{right} in the region to the left of L_{left} or to the right of L_{right}, respectively. If such contours exist, proceed to Step 3. Otherwise, the post bolt is determined to be missing, and the position information is recorded.

Step 3: Search for a closed contour within the identified closed contour that simultaneously satisfies the following two conditions. If such a contour exists, the post bolt is determined to be not missing. Otherwise, the post bolt is determined to be missing, and the position information is recorded.

① The size of the closed contour satisfies the specified requirements.

② When mapped to ImgM, the color inside the closed contour is consistent with the color in the region between L_{left} and L_{right}.

For square tube posts, the missing bolts were detected from $ImgM_{edge}$ according to the following steps:

Step 1: Select the top region between L_{left} and L_{right} as the key region.

Step 2: Identify hexagonal contours satisfying the specified size requirements within the key region, and count the number of hexagonal contours as k1.

Step 3: Identify concentric circular contours and concentric elliptical contours satisfying the specified size requirements within the key region. Count the number of concentric circular contours and concentric elliptical contours, and define their sum as k2.

ISSN 2616-5767 Vol.9, Issue 4: 82-89, DOI: 10.25236/AJETS.2026.090410

Step 4: Determine whether k1+k2=2 is satisfied. If yes, the post bolts are determined to be not missing. Otherwise, the post bolts are determined to be missing, and the position information is recorded.

4.6 Post Cap Missing Detection

For circular tube posts, determine whether $ImgM_{edge}$ simultaneously satisfies the following two conditions:

(1) No contour connected with L_{left} or L_{right} exists in the top region on the left side of L_{left} or the right side of L_{right};

(2) Two concentric circular contours or two concentric elliptical contours exist at the top of the region between L_{left} and L_{right}, and the size ratio between the two concentric contours satisfies the specified requirements.

If both conditions are satisfied, the post cap is determined to be missing, and the position information is recorded. Otherwise, the post cap is determined to be not missing.

5. Experimental Testing

To verify the feasibility of the proposed detection technology, a vehicle-mounted vision system was first constructed. Three color line-scan industrial cameras with a resolution of 4K pixels and a line rate of 10,000 lines/s were used to acquire images of the guardrail panels from the front-view, top-view, and bottom-view perspectives, respectively. A 20-megapixel color area-scan industrial camera was used to acquire images of the posts and their bolts on the outer side of the guardrail. Meanwhile, an incremental encoder with an output of 1,000 pulses per revolution and a vehicle-mounted GPS positioning module were employed as position-sensing devices for the inspection vehicle. An Advantech industrial computer was equipped as the core control unit.

Based on the vehicle-mounted vision system described above and the guardrail surface defect detection method proposed in this study, dedicated software was developed using the Microsoft Visual Studio 2019 development platform and the VC++ programming language. The inspection vehicle traveled at a speed of 40 km/h to acquire images and position information of roadside guardrails at the test site of the National Engineering Research Center for Mountainous Highways. Subsequently, guardrail panel bolt missing detection, guardrail panel top/bottom edge deformation damage detection, internal deformation damage detection of guardrail panel surfaces, post bolt detection, and post cap missing detection were performed. Among these tests, the panel bolts of the three-wave corrugated beam steel guardrail were automatically identified in the images acquired by the three line-scan industrial cameras, respectively. The identification results were then combined and displayed in the front-view image of the guardrail panel acquired by the No. 1 line-scan industrial camera. Typical results are shown in Fig. 3. Typical results of automatic bolt identification for square tube posts of the three-wave corrugated beam steel guardrail are shown in Fig. 4.



Fig. 3 Typical results of automatic guardrail panel bolt identification

ISSN 2616-5767 Vol.9, Issue 4: 82-89, DOI: 10.25236/AJETS.2026.090410



Fig. 4 Typical results of automatic post bolt identification

As shown in Fig. 3, even in regions with relatively dense bolt distributions, such as the joints of three-wave guardrail panels, the vehicle-mounted vision system can clearly acquire complete images of the guardrail panel surfaces. Meanwhile, the proposed detection method can accurately identify and mark all bolts on the guardrail panel surfaces, providing a solid foundation for determining whether panel bolts are missing. As shown in Fig. 4, the images of the posts and their bolts acquired by the area-scan industrial camera are also very clear. Using the proposed detection method, the bolt heads on the side with hexagonal contours and the nuts on the side with concentric elliptical contours were accurately identified and marked. No misidentification of concentric elliptical contours as two separate bolts occurred.

6. Conclusion

Focusing on the practical requirements for surface defect detection of corrugated beam steel guardrails, this study addressed the limitations of traditional manual inspection methods, including low efficiency, poor accuracy, high labor intensity, and insufficient operational safety. A systematic investigation was conducted involving the design scheme of a vehicle-mounted vision system, component selection, layout optimization, and the development of a complete surface defect detection method. Ultimately, an efficient, reliable, and automated technical solution for guardrail surface defect detection was established.

The proposed method enables accurate identification and localization of major surface defects, including guardrail panel deformation, missing bolts, missing post bolts, and missing post caps. It significantly improves the efficiency and quality of highway traffic safety facility monitoring, effectively reduces the cost and operational risks associated with manual inspection, and can be widely applied to routine guardrail monitoring and safety hazard investigation on various types of roads, including expressways and ordinary highways.

Meanwhile, this study still has certain limitations. Future research should further optimize image preprocessing algorithms to improve defect detection accuracy under complex road conditions such as strong sunlight, heavy rain, and dense fog. In addition, the capability of the system to identify subtle defects such as scratches and corrosion should be expanded. These efforts will promote the development of highway guardrail inspection technology toward intelligent, integrated, and all-weather operation, thereby providing more comprehensive and effective technical support for highway traffic safety assurance.

References

[1] Ma S. Y., Luo L. Research on an Intelligent Diagnostic System for Expressway Guardrail Defects Empowered by an Edge-Deployed Large Model[J]. Western China Communications Science & Technology, 2026, (5): 237–240.

[2] Li Z. X., Zhang H., Zhang C. L., et al. Missing-Bolt Detection in Highway Corrugated Steel Beam Guardrails Using a Lightweight Improved YOLOv8 Algorithm[J]. Wuhan University Journal of Natural Sciences, 2026, 31(4): 380–390.

ISSN 2616-5767 Vol.9, Issue 4: 82-89, DOI: 10.25236/AJETS.2026.090410

[3] Wei L., Wei Z. T., Shi J. M., et al. Rapid Detection Technology for the Extent of Damage to Expressway Corrugated Beam Guardrails[J]. Transportation Science & Technology and Management, 2026, 7(11): 87–89.
[4] Wang H. F., Guan Y. Y., Bai J. D., et al. Multi-Parameter Detection Robot System for Highway Corrugated Beam Steel Guardrail Based on Linear Structured Light Scanning[J/OL]. Journal of Traffic and Transportation Engineering. https://doi.org/10.19818/j.cnki.1671-1637.2026.278.
[5] Li S. Design and Application of a Highway Corrugated Beam Guardrail Damage Detection System[J]. Transportation Science & Technology and Management, 2025, 6(15): 7–9.
[6] Li J. Damage Detection System for Highway Corrugated Beam Guardrails Based on Machine Vision[D]. Tianjin University of Science & Technology, 2022.
[7] Yang M., Dang Q., Wan J. Intelligent Monitoring System for Highway Guardrail Conditions Based on Machine Vision[J]. China ITS Journal, 2023, (S1): 250–254.